

Electronic and optical properties of ZnO: first principle investigations

Faycal Baira¹, Sara Zidani²

¹Department of Sciences and technology, Faculty of technology, University of Batna 2, Alleys 53, Constantine Avenue. Fésdis, Batna 05078, Algeria

²Department of Food Technology, Laboratory of Food Science (LSA), Institute of Veterinary and Agricultural Sciences, University of Batna 1 Hadj Lakhdar, Alleys May 19 Biskra Avenue, Batna, 05000, Algeria

Author Correspondence email: f.baira@univ-batna2.dz

Received 10 March, 2023. Accepted 22 May, 2023. Published 13 July, 2023

Abstract:

Dielectric function and optical properties of oxide zinc (ZnO) nanostructure are studied by the first-principle computational within the framework of the density functional theory (DFT) using SIESTA code. The calculated lattice parameters and internal coordinates are in very good agreement with the experimental findings. Band structure, PDOS, real and imaginary parts of dielectric function, reflectance and absorbance has been calculated. A comparison with the previous studies has been made.

Keywords: Density Functional Theory, Siesta, Optical properties, Dielectric function.

Tob Regul Sci. TM 2023;9(1): 3654-3662

DOI: doi.org/10.18001/TRS.9.1.256

1. Introduction

Zinc oxide is a direct wide band gap ($\Delta E = 3.37$ eV) semiconductor with a large excitation binding energy of 60 meV, which makes ZnO an attractive versatile material applied in

Photodiodes [1], photocatalysis [2], sensing [3-4] and photovoltaic cells [5-6]. Mesoporous materials have found a large number of significant benefits due to their large surface area and well organized porous mesostructure. The physical properties of mesoporous ZnO could be improved leading to high optical quality, low refractive index, photoluminescent, small crystal sizes and better photocatalytic activity [7].

The no central symmetry and the tetrahedral coordinated ZnO unit in ZnO result in anisotropic piezoelectric properties. Structurally, the wurtzite structured ZnO crystal is described schematically as a number of alternating planes composed of four-fold coordinated O^{2-} and Zn^{2+} ions, stacked alternatively along the c-axis. The oppositely charged ions produce positively charged (0001)-Zn and negatively charged ($000\bar{1}$)-O polar surfaces, resulting in a normal dipole moment and spontaneous polarization as well as a divergence in surface energy. To maintain a

stable structure, the polar surfaces generally have facets or exhibit massive surface reconstructions, but ZnO (0001) is an exception, which is atomically flat, stable, and without reconstruction [8-9]. Understanding the superior stability of the ZnO (0001) polar surfaces is a forefront research in today's surface physics [10-13].

Transparent conducting zinc oxide (ZnO) thin films have extensively studied in the last years due to their interesting properties such as high transmission coefficient in visible and high reflection of infrared radiation, direct optical band-to-band transitions, low electrical resistivity, etc [14-21].

In this paper, we use density-functional theory (DFT) to investigate the structural, electronic, and optical properties of the ZnO nanostructure. The study may provide some useful information for future investigations in oxide metal catalysts.

2. Computational details

Our calculations are performed by using the first-principles pseudo potential method based on density functional theory (DFT) within the generalized gradient approximation (GGA) as implemented in the SIESTA [22,23]. The GGA-PBE exchange-correlation functional, as parameterized by Wang, Perdew and Ernzerhof, is employed [24]. In the case of LCAO calculations (Siesta), the pseudo potentials reconstructed by the Troullier–Martins scheme [25]. The double- ζ plus polarization basis set search for Zn, O respectively. A real space mesh cutoff of 300 Ry and a reciprocal space grid cut off of approximately 15\AA was used. The structure relaxation was done using the conjugated gradient method until the Hellman Feynman force on each atom is smaller than 0.05 eV/\AA .

The Gamma centered grid of $(6 \times 6 \times 1)$ k points was used for the Brillouin zone integration during geometry relaxation. To calculate the optical properties, a grid of $(9 \times 9 \times 1)$ k points was used. For the bulk ZnO, the calculated lattice constants are 3.284 and 5.330 \AA , which are in reasonable agreement with the corresponding experimental values 3.250 and 5.207 \AA [26].

3. Results and discussion

a. Unit cell structure

Unit cell structure ZnO stable (B4) structure having hexagonal primitive unit cell with space group $C4_6v P6_3mc$. Each primitive unit cell of ZnO consists of four atoms where two Zn atoms are at the positions $(1/3, 2/3, 0)$, $(1/3, 2/3, 1/2)$ and O atoms at positions $(1/3, 2/3, \mu)$, $(1/3, 2/3, \mu + 1/2)$. μ is the internal parameter of the B4 phase that determines the bond-length (anion_cation bond length) parallel to c-axis divided by the c-lattice parameter.

$$\mu = \left(\frac{1}{4} + \left(\frac{c^2}{3a^2} \right) \right)$$

(1)

The bulk parameters of ZnO are calculated to be $a = 3.284 \text{ \AA}$, $c = 5.330 \text{ \AA}$, and $E_g = 0.65 \text{ eV}$ which is in reasonable agreement with the previous DFT calculation with $a = 3.283 \text{ \AA}$, $c = 5.289 \text{ \AA}$ [27]. Table 1 shows the results of a , b , c/a and band gap (E_g).

Table 1: The calculated lattice parameters of ZnO in phase (wurtzite) in comparison with theoretical values available.

Methode	Code	$a \text{ (\AA)}$	$c \text{ (\AA)}$	c/a	$E_g \text{ (ev)}$
This work	Siesta: GGA	3.284	5.330	1.623	0.65
Ref [28]	Transiesta: GGA	3.288	5.270	1.603	1.02
Ref [29]	Wien2k: GGA	3.300	5.346	1.620	0.69
Ref [30]	Wien2k: GGA	3.240	5.200	1.602	1.20

Our results with GGA are in good agreement to another theory Results [28-30], which is lower than the experimental value in band gap. This is regarded as a spread problem of DFT calculations.

B. Band structure and density of states

The band structure of ZnO in wurtzite is evaluated using calculated lattice parameters ($a = 3.284 \text{ \AA}$, $c = 5.330 \text{ \AA}$). It can be seen that the valence band maxima and conduction band minima lie on the same Γ point, indicating direct band with value 0.65 eV .

Calculated band gap values with GGA are smaller than experimental results indicating that this form of GGA is not sufficiently flexible to give consistent results for band gap energy similar to other forms of GGAs and LDA. Our calculated band gap value for wurtzite is about 60.00% less than that of experimentally [31], reported band gap values. This is in good agreement with Similar to the result of the theory [30]. The band structure show in figure 1.

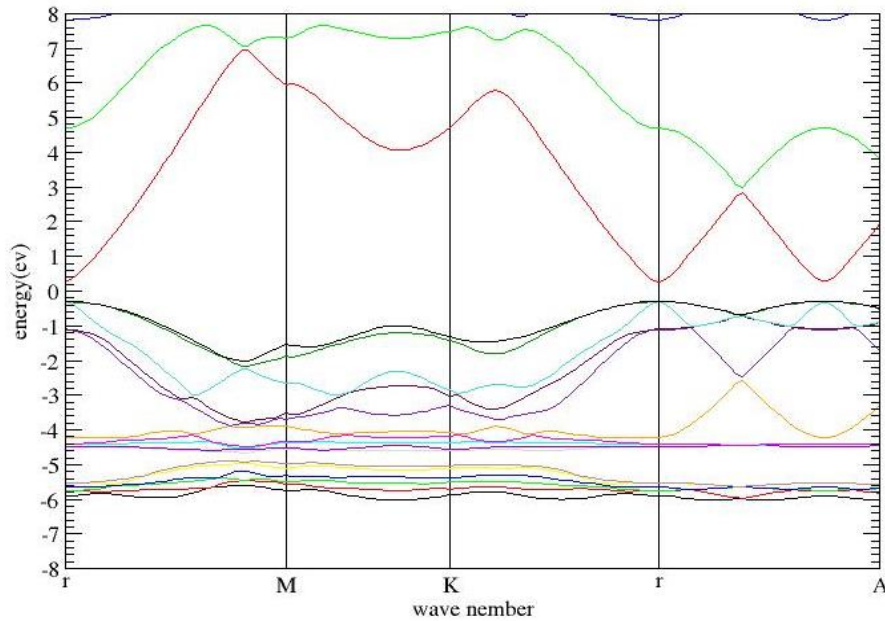


Figure 1: Band structure of ZnO for wurtzite.

C. Density of states

We will calculate the partial densities of states of zinc and oxygen elements that contribute to the total density of states of ZnO in the solid state. We will explain it in detail to understand the movement of electrons near Fermi level. Figure 2 shows the partial densities of states of ZnO.

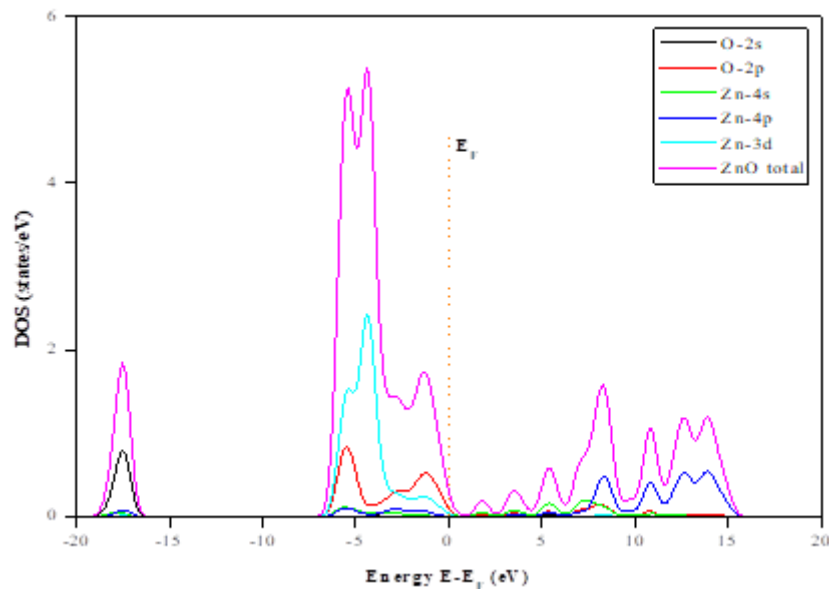


Figure 2: Partial DOS (states/eV).

From figure 2, We can say that the presence of density of states peaks in the valence band region is mainly due to the 3d state of the zinc element (Zn) and the p state of the oxygen element (O), while the small peaks observed within the conduction band region are essentially due to the p state of the zinc (Zn) and the participation of s and p states of the zinc (Zn) and (O).

Respectively. Therefore, d state of zinc and p state of oxygen are the cause of the presence of the density of the state in the valence band region but the contribution of d state is predominant.

We can also see the emergence of bonding level near the Fermi level at energy of -1.8 eV and also an anti-bonding level near to energy of 2 eV, which makes the possibility of electron transmission from the valence band to the conduction band if the oxide is exposed to external stimulation such as light.

D. Optical Properties

Optical properties play an active role in the understanding of the nature of material and provide a clear picture for the usage of a material in optoelectronic devices. It is generally known that the interaction of a photon with the electrons in the system can be described in terms of time dependent perturbations of the ground-state electronic states. Transitions between occupied and unoccupied states are originated by the electric field of the photon. The optical response of a material to the electromagnetic field at all energy levels, can be described by means of complex dielectric function $\epsilon(\omega)$ as,

$$\epsilon(\omega) = \epsilon_1(\omega) + i\epsilon_2(\omega) \quad (2)$$

Where, $\epsilon_1(\omega)$ and $\epsilon_2(\omega)$ are real and imaginary part of the dielectric function. Real part of the dielectric function $\epsilon_1(\omega)$, means the dispersion of the incident photons by the material, while the imaginary part of the dielectric function $\epsilon_2(\omega)$, corresponds to the energy absorbed by the material. There are two contributions to complex dielectric function $\epsilon(\omega)$, namely intraband and interband transitions. The contribution from intraband transitions is influential only for metals. The interband transitions can be further divided into direct and indirect transitions [20,32]. The imaginary part $\epsilon_2(\omega)$ of the dielectric function is calculated from the contribution of the direct interband transitions from the occupied to unoccupied states and the calculation is associated with the energy eigen value and energy wave functions, which are the direct output of band structure calculation.

The figure 3 shows the plot of real and imaginary part of dielectric function.

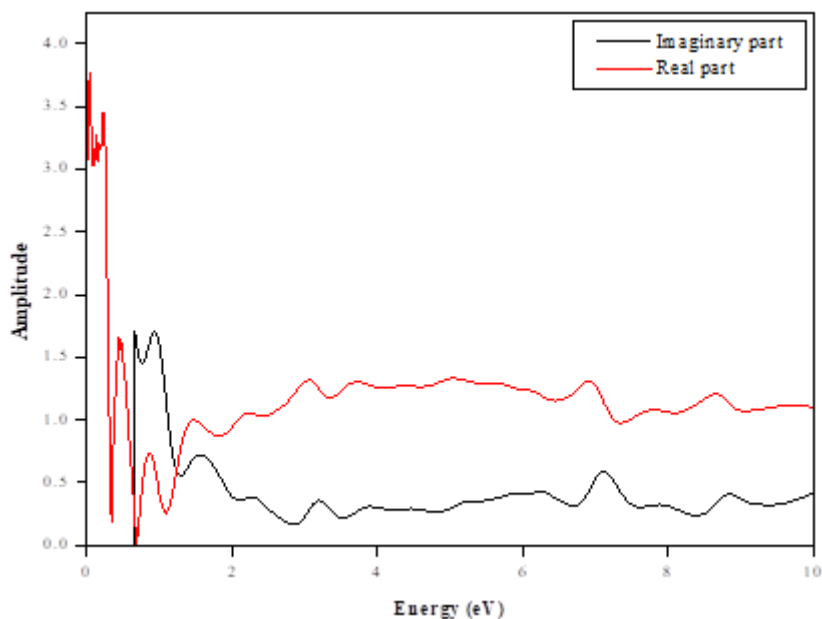


Figure 3: Real and Imaginary part of dielectric function.

The imaginary part of the dielectric tensor can be computed by the knowledge of the electronic band structure of the solid. The imaginary part of the dielectric function, as displayed indicate that, there is no optical adsorption in the low-energy region (0-0.65 eV) for both polarizations but for further energies, there is optical adsorption and strong anisotropy in the optical spectra.

E. Reflectance and Absorption

The reflectance and absorption values of the ZnO have been calculated. Figure 4 shows that the reflectance values increase with wavelength in the range of [1130-1500] nm until reaches its highest value at wavelength 1200 nm, It also decrease to reaches very small values of approximately 4% of the value of the beam received within the visible rang. The same Figure shows the absorption of this oxide, which is similar to that found by V. Jan-Christoph Deinert [29,33], where the absorption of radiation for this oxide is high in infrared region and reaches, its maximum in the range of [1350-1200] nm. This makes the ZnO suitable for use as an infrared detector and at the same time as conductor if the absorbed energy of these wavelengths is greater than its gap energy. Then, their values decrease to a wavelength of 950 nm and rise a little in a small wavelength range, afterward it regresses again.

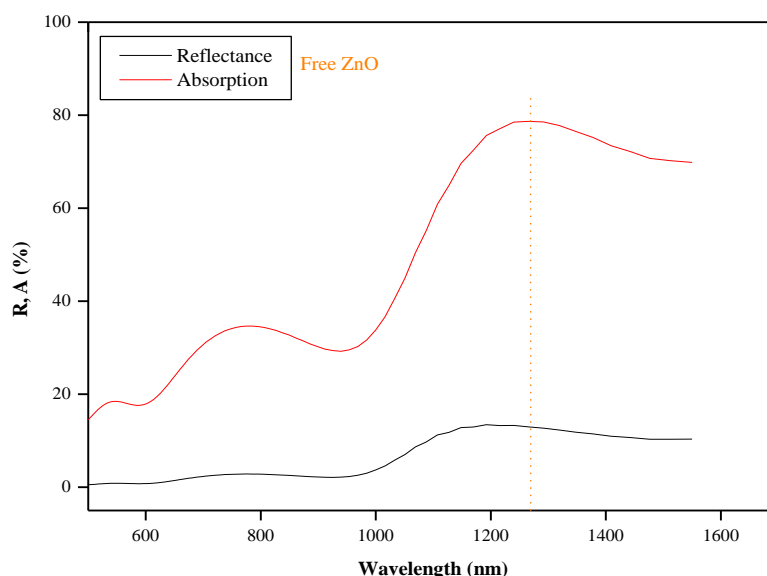


Figure 4: Absorption and reflectance as a function of the wavelength of ZnO.

References

1. J.Y. Lee, Y.S. Choi, J.H. Kim, M.O. Park, S. Im, Optimizing n-ZnO/p-Si heterojunctions for photodiode applications, *Thin Solid Films*. **553**, 403-404 (2002).
2. O.A. Fouad, A.A. Ismail, Z.I. Zaki, R.M. Mohamed, Zinc oxide thin films prepared by thermal evaporation deposition and its photocatalytic activity. *Appl. Catal. B: Environ.* **62**(1), 144-149 (2006).
3. J. Rao, A. Yu, C. Shao, X. Zhou, Construction of Hollow and Mesoporous ZnO Microsphere: A Facile Synthesis and Sensing Property. *ACS Appl. Mater. Interfaces*. **4**(10) 5346-5352 (2012).
4. A.M. Ali, A.A. Ismail, R. Najmy, A. Al-Hajry, Annealing effects on zinc oxide-silica films prepared by sol-gel technique for chemical sensing applications. *Thin Solid Films*. **558**, 378-384 (2014).
5. R. Tena-Zaera, A. Katty, S. Bastide, C. Levy-Clement, Annealing Effects on the Physical Properties of Electrodeposited ZnO/CdSe Core-Shell Nanowire Arrays. *Chem. Mater.* **19**(7), 1626-1632 (2007).
6. Y. Qin, X. Wang, Z.L. Wang, Microfibre-nanowire hybrid structure for energy scavenging. *Nature*. **451**, 809-813 (2008).
7. S. Lepoutre, B. JulianLopez, C. Sanchez, H. Amenitsch, M. Lindend, D. Grosso, Nanocasted mesoporous nanocrystalline ZnO thin films. *J.Mater. Chem.* **20**(3), 537-542 (2010).
8. Dulub, O.; Boatner, L. A.; Diebold, U. STM study of the geometric and electronic structure of ZnO(0001)-Zn, (000-1)-O, (10-10), and (11-20) surfaces. *Surf. Sci.* **519**, 201-217 (2002).

9. Meyer, B.; Marx, D. Density-functional study of the structure and stability of ZnO surfaces. *Phys. Rev. B*. **67**, 035403 (2003).
10. Tasker, P. W. The stability of ionic crystal surfaces. *J. Phys. C: Solid State Phys.* **12**(22), 4977-4984 (1979).
11. Dulub, O.; Diebold, U.; Kresse, G. Novel Stabilization Mechanism on Polar Surfaces: ZnO(0001)-Zn. *Phys. Rev. Lett.* **90**(1), 016102-4 (2003).
12. Wander, A.; Schedin, F.; Steadman, P.; Norris, A.; McGrath, R.; Turner, T. S.; Thornton, G.; Harrison, N. M. Stability of Polar Oxide Surfaces. *Phys. Rev. Lett.* **86**, 3811 (2001).
13. V. Staemmler, K. Fink, B. Meyer, D. Marx, M. Kunat, S. Gil Girol, U. Burghaus, Ch. Wo"ll, Stabilization of Polar ZnO Surfaces: Validating Microscopic Models by Using CO as a Probe. *Molecule. Phys. Rev. Lett.* **90**, 106102 (2003).
14. G. Harbeke (ed.), Polycrystalline Semiconductors: Physical Properties and Applications (Springer-Verlag, Berlin,), pp. 244-314 (1985).
15. K. L. Chopra and S. R. Das, Thin-Film Solar Cells (Plenum Press, New York, pp. 67-88 (1983).
16. H. L. Hartnagel, A. L. Dawar, A. K. Jain and C. Jagadish, Semiconducting Transparent Thin Films (IOP Publishing, Bristol and Philadelphia, (1995).
17. F. C. M. Van Pol, F. R. Blom and Th. J. Popma, R.F. planar magnetron sputtered ZnO films I: structural properties. *Thin Solid Films* **204**, 349-364 (1991).
18. F.R. Blom, F. C. M. Van Pol, G. Bauhvis and Th. J. A. Popma, R.F. planar magnetron sputtered ZnO films II: Electrical properties Thin Solid Films **204**(2), 365-376 (1991).
19. P. Baranski, V. Klotchkov and I. Potykevich, Electronique des Semiconducteurs Mir, Moscou, (1978).
20. K. Ellmer and R. Mientus, Carrier transport in polycrystalline transparent conductive oxides: A comparative study of zinc oxide and indium oxide. *Thin Solid Films*. **516**(14), 4620-4627 (2008).
21. N. Tsuda, K. Nasu, A. Fujimori and K. Siratori, Electronic Conduction in Oxides (Springer, Berlin-Heidelberg, 2000).
22. D. Sánchez- Portal, P. Ordejón, E. Artacho, J.M. Soler, Density functional method for very large systems with LCAO basis sets, *Int. J. Quant. Chem.* **65**(5), 453 (1997).
23. PaoloGiannozzi,Quantum-ESPRESSOisaCommunityProjectforHigh-quality Quantum-simulation Soft ware, Based on Density-functionalTheory. ([http:// www.quantum-espresso.org](http://www.quantum-espresso.org) and <http://www.pwscf.org>).
24. J.P. Perdew, K.Burke, M.Ernzerhof, Generalized gradient approximation made simple, *Phys.Rev.Lett.***77**, 3865-3868 (1996).
25. N. Troullier, J.L.Martins, Efficient pseudopotentials for plane-wave calculations, *Phys.Rev.B***43**, 1993-2006 (1991).

26. C.H. Bates, W.B. White, R. Roy, New High-Pressure Polymorph of Zinc Oxide. *Science* **137(3534)**, 993 (1962).
 27. A. Schleife, F. Fuchs, J. Furthmuller, F. Bechstedt,. First-principles studies of ground- and excited-state properties of MgO, ZnO, and CdO polymorphs. *Phys. Rev. B.* **73**, 245212-13 (2006),
 28. A. Srivastava, N.Tyagi, Pressure Induced Phase Transition and Electronic Properties of 1d ZnO Nanocrystal: AN AB INITIO Study. *J. Phys. World Scientific.* **11(5)**, 1250035 (2012).
 29. A. Mokadem, M. Bouslama, O. Benhelal, A. Assali, M. Ghaffour, Z. Chelahi Chikr, K. Boulenouar, A.Boubaia, Investigation of the electron structure of ZnO by the GGA and mBJ calculations associated with the characterization techniques AES and EELS .*J. Phys. World Scientific.*, 28(11), 1250035-11 (2014).
 30. B. Ul haq, A. Afaq, R. ahmed, S. naseem, A COMPREHENSIVE DFT STUDY OF ZINC OXIDE IN DIFFERENT PHASES.*Int. J. Mod. Phys C.* **23(6)**, 20121250043-10.
 31. J.A. Camargo-Martínez and R. Baquero, The band gap problem: the accuracy of the Wien2k code Confronted. **59**, 453-460 (2013).
 33. V. Jan-Christoph Deinert, Zinc Oxide Surfaces and Interfaces: Electronic Structure and Dynamics of Excited States. Theses PhD (2016).
-